Pergamon

*Computers Math. Applic.* Vol. 29, No. 6, pp. 99–108, 1995

0898-1221/95 $9.50 + 0.00

**0898-1221(95)00011-9**

# Thermal Transport of a Continuous Moving Plate in a Non-Newtonian Fluid

SO-YENN TSAI
Department of Tool and Die-Making
National Kaohsiung Institute of Technology, Kaohsiung, Taiwan, 80782, R.O.C.

TSAN-HUI HSU
Department of Mechanical Engineering
National Kaohsiung Institute of Technology, Kaohsiung, Taiwan, 80782, R.O.C.

*(Received July 1993; accepted August 1993)*

**Abstract**—The phenomena of conjugate convection-conduction heat transfer of a non-Newtonian fluid on a continuous moving flat plate were investigated numerically. The self-induced forced convection heat transfer in this study reveals some significantly different characteristics. Of particular interest were the effects of power-law viscosity index, generalized Prandtl number, and material parameter on the heat transfer characteristics and temperature distribution on the plate. The temperature level is found to decay gradually with distance along the moving surface. The local Nusselt number increases monotonically with the distance and eventually attains a constant value. The skin friction coefficient on the wall displays quite different features for the present fluids.

## NOMENCLATURE

| | |
|---|---|
| $C$ | specific heat of the fluid |
| $C_f$ | skin friction coefficient |
| $C_p$ | specific heat of the plate |
| $h$ | heat transfer coefficient |
| $K$ | consistency index |
| $k$ | thermal conductivity of the fluid |
| $k_p$ | thermal conductivity of the plate |
| $L$ | length of the plate |
| $\mathrm{Nu}_x$ | local Nusselt number, $hx/k$ |
| Pe | Peclet number, $U_w\,\delta^2/(\alpha_p L)$ |
| Pr | generalized Prandtl number, $\frac{L\,U_w}{\alpha}\,\mathrm{Re}^{-2/(n+1)}$ |
| $R$ | property parameter, $\left(\frac{k\rho\,C}{k_p\,\rho_p\,C_p}\right)^{1/2}$ |
| Re | Reynolds number, $\frac{\rho U_w^{2-n} L^n}{K}$ |
| $T$ | temperature of the fluid |
| $T_0$ | temperature of the plate at the slot |
| $T_p$ | temperature of the plate |
| $T_\infty$ | ambient temperature of the fluid |
| $U,\ V$ | dimensionless velocities |
| $u,\ v$ | velocity components |
| $X,\ Y$ | dimensionless coordinates |
| $x,\ y$ | coordinates |
| $y_p$ | $y$-distance within the plate |
| $\alpha$ | thermal diffusivity |
| $\theta$ | dimensionless temperature of the fluid, $(T - T_\infty)/(T_0 - t_\infty)$ |
| $\delta$ | half thickness of the plate |
| $\rho$ | density |
| Subscripts | |
| $p$ | condition at the plate |
| $w$ | condition at the wall |
| $\infty$ | condition at freestream |

Typeset by $\mathcal{A}\mathcal{M}\mathcal{S}$-TEX

# INTRODUCTION

The problem of heat transfer on a continuous moving surface has many technical applications in industrial manufacturing. Well-known examples are rolling sheet drawn from a die, cooling and/or drying of paper and textile, manufacturing of polymeric sheets, sheet glass and crystalline materials. Sakiadis [1–3] was the first to introduce the concept of continuous moving surface. Due to the entrainment of ambient fluid, this situation represents a different class of boundary layer problem which has a solution substantially different from that of boundary flow over a stationary surface. Tsou *et al.* [4] extended the research to include the heat transfer phenomenon. The combined forced and free convection adjacent to continuous, moving sheets was studied numerically by Chen and Strobel [5] for a horizontal geometry and by Moutsoglou and Chen [6] for an inclined geometry. It is concluded that a positive buoyancy force contributes to an increase in the local friction factor and the local Nusselt number in these two studies. More recently, the analysis of conjugate heat transfer on a continuous moving surface has been investigated by many authors [7–12]. Erickson [7] studied the cooling of a moving continuous flat sheet. Grubka and Bobba [8] investigated heat transfer characteristics of a continuous, stretching surface with variable temperature. Chida and Katto [9] analyzed the conjugate heat transfer of continuous moving surfaces, and verified the analytical results by measurement. In addition, Karwe and Jaluria [10,11] presented the fluid flow and mixed convection transfer from a moving plate. The results obtained were compared with those for the idealized cases of an assumed surface heat transfer coefficient and of a moving isothermal surface.

Recently, the problem of non-Newtonian fluids has received considerable attention because of the wide use of these fluids in chemical process industries, food engineering, petroleum production, and power engineering. Many of the non-Newtonian fluids encountered in chemical engineering processes are known to follow the empirical Ostwald-de Waele power-law model. Valuable contributions to the problem of a moving surface in this fluid have been investigated. Char and Chen [12] studied the temperature field of such fluid over a stretching plate with varied heat flux. Pop *et al.* [13] presented the heat transfer of non-Newtonian fluids on a moving cylinder for both constant wall temperature and constant wall heat flux. A second-order boundary layer solution for such subjects was investigated by Pop and Gorla [14]. It was pointed out that the generalized Prandtl number and power-law viscosity index affect the flow field to a large extent.

The conjugate problem including convection and conduction is of more practical importance. In addition, in most practical cases, interest lies mainly in the temperature distribution and heat trasfer coefficient on the moving surface. The effects of the power-law viscosity index, the generalized Prandtl number, Peclet number, and material parameter on the temperature distribution, as well as the local Nusselt number were discussed in the present study. Numerical solutions were carried out for pseudoplastic fluids ($n < 1$), Newtonian fluids ($n = 1$), and dilatant fluids ($n > 1$) with $\mathrm{Pr} = 10$ to 100.

# ANALYSIS

Consider a continuous horizontal flat plate with thickness $2\delta$, which is emerged from a slot at fixed temperature $T_0$ and is continuously moving with steady velocity $U_w$ in an otherwise quiescent non-Newtonian fluid with temperature $T_\infty$ (Figure 1).

Two different stationary axes are chosen with the origin located at the slot. The positive $x$ axis extends parallel to the plate and in the direction of its motion. The $y$ axis for the fluid is outside the plate; the one for the plate is within the plate and is denoted by $y_p$. The two $y$ scales originate at the slot and extend upwards. Viscous dissipation is neglected in the energy equation. The fluids are assumed to follow the Ostwald-de Waele power-law model. The boundary layer

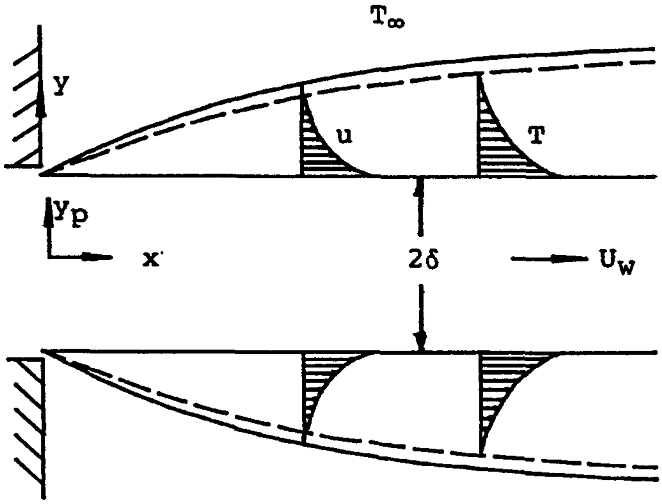


Figure 1. Schematic diagram of the system.

equation may be expressed in dimensionless form as

$$\frac{\partial U}{\partial X} + \frac{\partial V}{\partial Y} = 0, \tag{1}$$

$$U \frac{\partial U}{\partial X} + V \frac{\partial U}{\partial Y} = \frac{\partial}{\partial Y}\left(\left|\frac{\partial U}{\partial Y}\right|^{n-1} \frac{\partial U}{\partial Y}\right), \tag{2}$$

$$U \frac{\partial \theta}{\partial X} + V \frac{\partial \theta}{\partial Y} = \frac{1}{\Pr} \frac{\partial^2 \theta}{\partial Y^2}, \tag{3}$$

where Pr is the generalized Prandtl number, defined as

$$\Pr = \frac{L U_w}{\alpha} \mathrm{Re}^{-2/(n+1)}.$$

The boundary conditions for the flow field are

$$U = V = \theta = 0, \qquad X = 0, \quad Y > 0, \tag{4}$$

$$U = 1, \quad V = 0, \quad \theta = \theta_p(X, 1), \qquad X \geq 0, \quad Y = 0, \tag{5}$$

$$U \to 0, \quad \theta \to 0, \qquad X > 0, \quad Y \to \infty. \tag{6}$$

The flat plate is assumed to be of finite thickness and large width, as occurred in the extrusion process. According to the analysis of Karwe and Jaluria [10], the conduction in the plate is taken into account at present. The energy equation for the plate is

$$U_w \frac{\partial T_p}{\partial X} = \alpha_p \frac{\partial^2 T_p}{\partial Y_p^2}, \tag{7}$$

where $T_p$ and $\alpha_p$ are the temperature and thermal diffusivity of the plate, respectively.

Equation (7) may be rearranged in dimensionless form as

$$\frac{\partial \theta_p}{\partial X} = \frac{1}{\mathrm{Pe}} \frac{\partial^2 \theta_p}{\partial Y_p^2}, \tag{8}$$

with the corresponding boundary conditions

$$\theta_p(0, Y_p) = 1, \qquad X = 0, \tag{9}$$

$$\frac{\partial \theta_p}{\partial Y_p} = 0, \qquad X \geq 0, \quad Y_p = 0, \tag{10}$$

$$\frac{\partial \theta_p}{\partial Y_p} = R\sqrt{\mathrm{Pe}/\Pr}\, \left.\frac{\partial \theta}{\partial Y}\right|_{Y=0}, \qquad X > 0, \quad Y_p = 1, \tag{11}$$

where $R$ is the property parameter and Pe is the Peclet number defined, respectively, as

$$R = \sqrt{\frac{k \rho C}{k_p \rho_p C_p}} \quad \text{and} \quad \mathrm{Pe} = \frac{\delta^2 U_w}{\alpha_s L}.$$

The above equations, i.e., (1)–(3) and (8), are generalized by using the following nondimensionalization

$$X = \frac{x}{L}, \quad Y = \frac{x^{n+1}\sqrt{\mathrm{Re}}}{L}, \quad Y_p = \frac{y_p}{\delta},$$
$$U = \frac{u}{U_w}, \quad V = \frac{v^{n+1}\,\mathrm{Re}}{U_w}, \quad \theta = \frac{T - T_\infty}{T_0 - T_\infty}, \quad \theta_p = \frac{T_p - T_\infty}{T_0 - T_\infty}.$$

The local Nusselt number is given by

$$\mathrm{Nu}_x = \frac{h\,x}{k} = -\mathrm{Re}^{-1/(n+1)} \frac{X}{\theta_w} \left.\frac{\partial \theta}{\partial Y}\right|_{Y=0}, \tag{12}$$

where Re is the generalized Reynolds number defined as

$$\mathrm{Re} = \frac{\rho U_w^{2-n} L^n}{K}.$$

The skin friction coefficient is defined as

$$C_f = \frac{2\tau_w}{\rho U_w^2} = 2\,\mathrm{Re}^{-1/(n+1)} \left(\frac{\partial U}{\partial Y}\right)^n_{Y=0}. \tag{13}$$

## NUMERICAL PROCEDURE

The solutions to equations (1)–(3), (8) were solved by the cubic spline collocation method [15]. The $x$-direction space was divided into 31 steps. Whereas, the thermal boundary of the fluid and the half thickness of the plate were divided into 51 and 21 nonuniform steps, respectively. A smaller grid spacing of the mesh points in the neighborhood adjacent to the surface as well as to the origin portion of the moving plate was chosen.

Equations (1)–(3) and (8) are transformed into the following form:

$$\varphi_{ij}^{n+1} = F_{ij} + G_{ij}\, m_{\varphi_{ij}}^{n+1} + S_{ij}\, M_{\varphi_{ij}}^{n+1}, \tag{14}$$

in which $\varphi$ represents the functions $U$, $\theta$, and $\theta_p$; $m$ and $M$ are the first and second derivatives of $\varphi$; and $n$ is the number of false time steps.

Equation (14) may be rearranged in tridiagonal form as

$$A_{ij}\, \phi_{i,j-1}^{n+1} + B_{ij}\, \phi_{ij}^{n+1} + C_{ij}\, \phi_{i,j+1}^{n+1} = D_{ij}, \tag{15}$$

where $\phi$ refers to $U$, $\theta$, and $\theta_p$ or their first two derivatives. Equation (15) may be solved easily by the Thomas algorithm. The solutions are obtained when the following convergency criterion is satisfied

$$\left|\frac{\phi_{ij}^n - \phi_{ij}^{n-1}}{\phi_{\max}^n}\right| < 10^{-4}. \tag{16}$$

## RESULTS AND DISCUSSION

Numerical results were obtained for a flow index $n$ of 0.2, 0.5, 0.8 (pseudoplastic fluids), $n = 1$ (Newtonian fluid), and $n = 1.5$, 2 (dilatant fluids); Prandtl number Pr of 10, 50, and 100, and various material parameters.

Figures 2 and 3 display the surface temperature distribution and generalized Nusselt number for various fluids characterized by different power-law indices. The surface temperature is higher for pseudoplastic fluids ($n < 1$) than for dilatant fluids ($n > 1$). On the other hand, significantly different behaviour of the local Nusselt number is found for various fluids. The local Nusselt number is larger for dilatant fluids in the portion near the slot ($X = 0$). Then, as $X$ increases, the difference reduces quickly, and at certain $X$-values the local Nusselt numbers for pseudoplastic fluids exceed those of dilatant fluids. This phenomenon can explain the fact that the surface temperature is lower for dilatant fluids near the slot, whereas, the surface temperature difference gets smaller gradually between the two different fluids in the downstream portion. Furthermore, for each fluid, the Nusselt number is observed to approach a constant value as the distance from the slot increases. The effect of the generalized Prandtl number on the heat transfer coefficient is shown in Figure 4. As excepted, larger Prandtl numbers yield higher local Nusselt numbers.

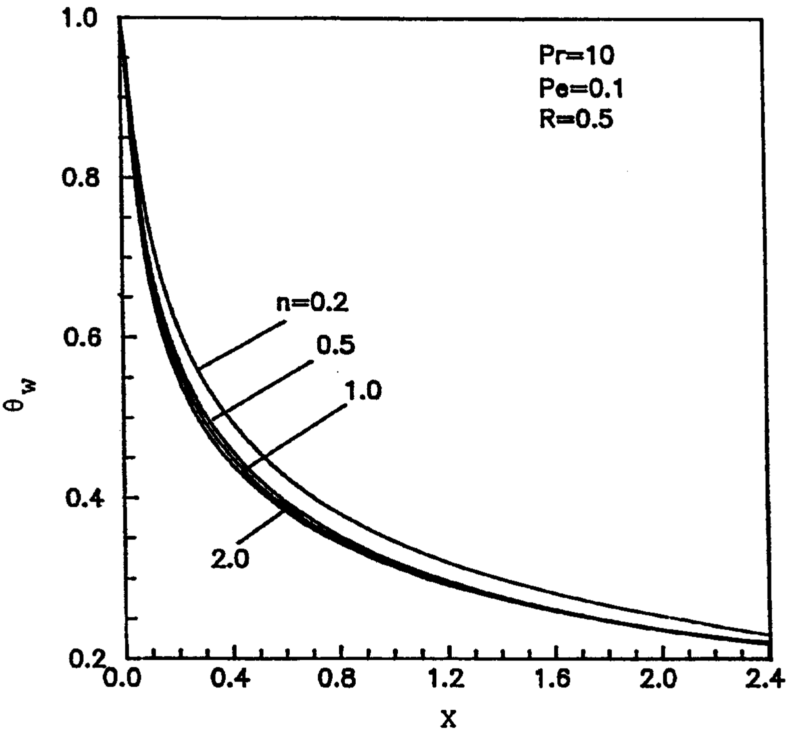


Figure 2. Effect of the viscosity index $n$ on the surface temperature distribution.

Figures 5 and 6 show the surface temperature distribution and heat transfer coefficient affected by the Peclet number Pe. For larger values of Pe, the plate is exposed for short durations to the cooler ambient fluids. Hence, less energy is lost from the surface. Therefore, larger values of Pe imply higher surface temperature and local Nusselt number.

The effect of the material parameter $R$ on the thermal field is illustrated in Figures 7 and 8. For smaller values of $R$, i.e., for a plate with high conductivity or large thermal capacity, the plate temperature drops very gradually. As a result, the local Nusselt numbers are also larger for smaller values of parameter $R$.

Figure 9 shows the variation of the skin friction coefficient with the distance along the plate. It is seen that the skin friction coefficient decreases monotonically along the surface. In the region near the slot, i.e., $X < 0.2$, the values of the skin friction coefficient are higher for dilatant

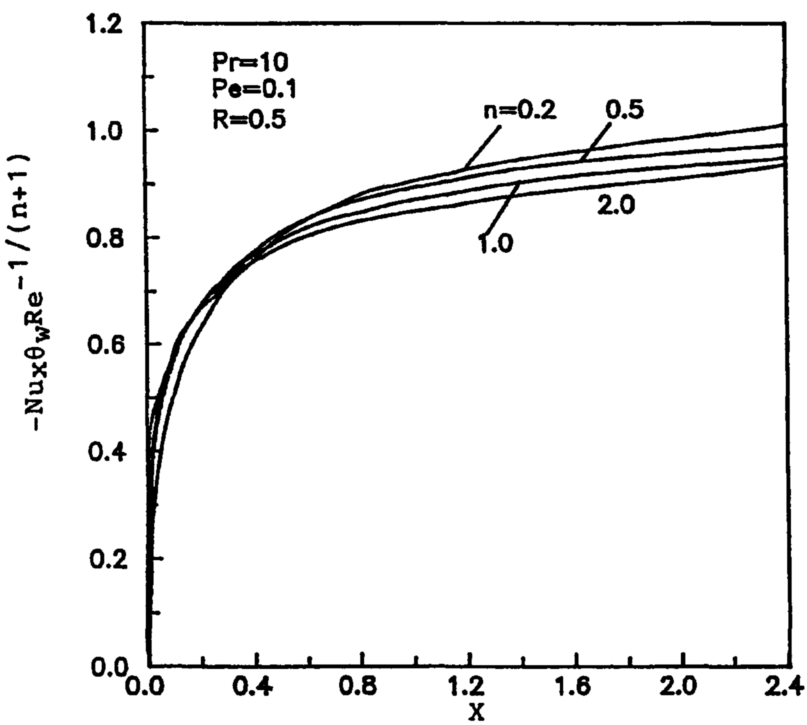


Figure 3. Local Nusselt number for different viscosity indices $n$.

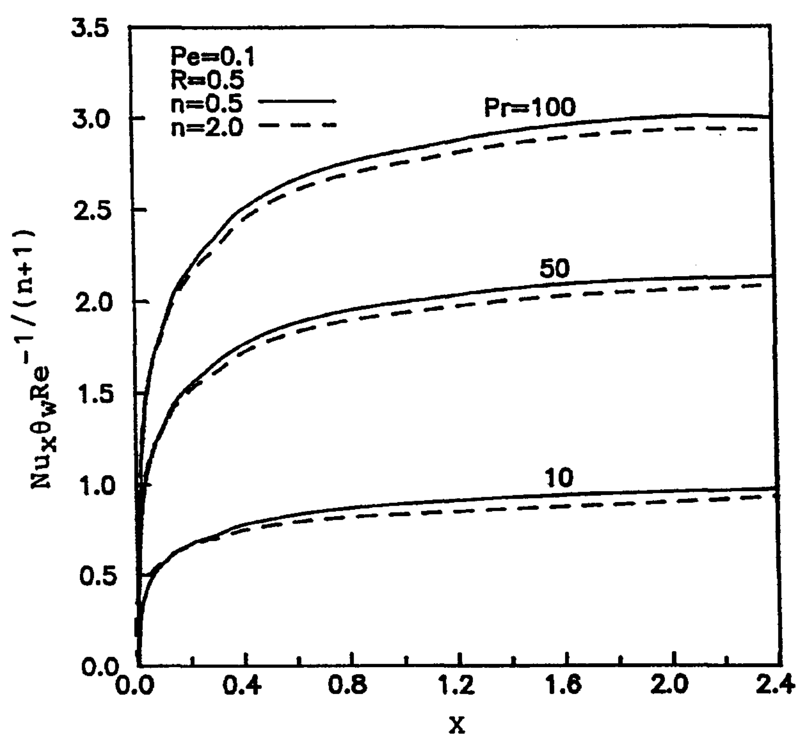


Figure 4. Effect of the Prandtl number Pr on the local Nusselt number.

fluids than for pseudoplastic fluids. On the other hand, a quite opposite behavior of the friction factor of both pseudoplastic and dilatant fluids is observed for $X > 0.2$. The velocity profiles for different fluids at $X = 2.4$ are shown in Figure 10. As expected, the velocity distribution is higher for pseudoplastic fluids and smaller for dilatant fluids.

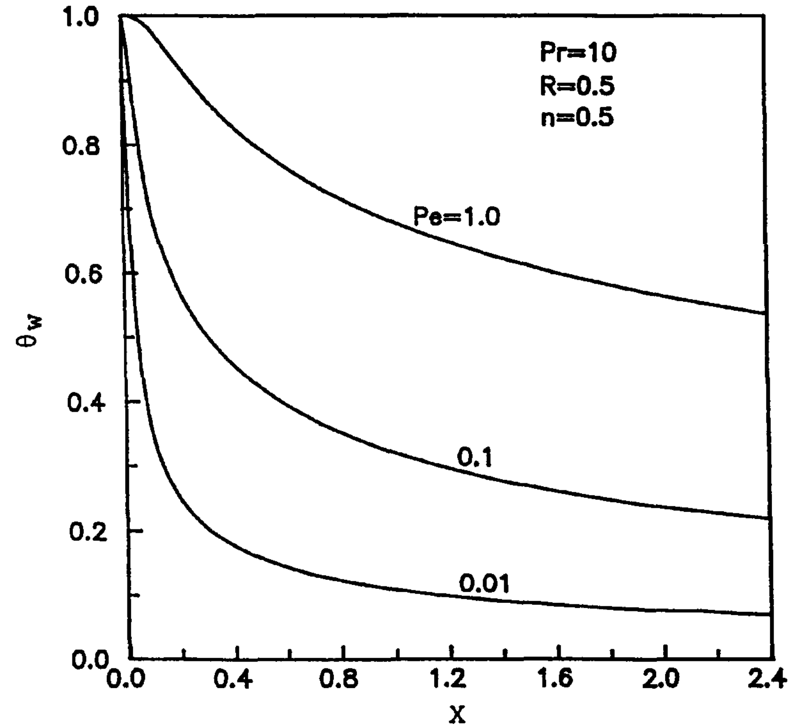


Figure 5. Effect of the Peclet number Pe on the surface temperature distribution.

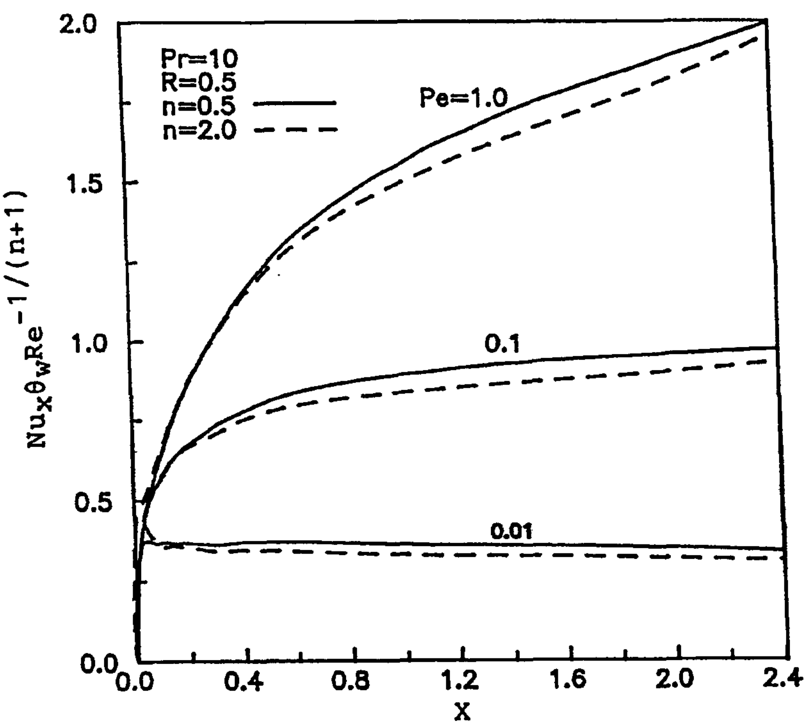


Figure 6. Local Nusselt number for different Peclet numbers Pe.

## CONCLUSION

The problem of the steady-state, self-induced forced convection heat transfer from a moving plate in power-law non-Newtonian fluids has been studied numerically using the cubic spline collocation method. The power-law index $n$ and generalized Prandtl number significantly influence both the flow and thermal fields. It is shown that the surface temperature distribution is lower

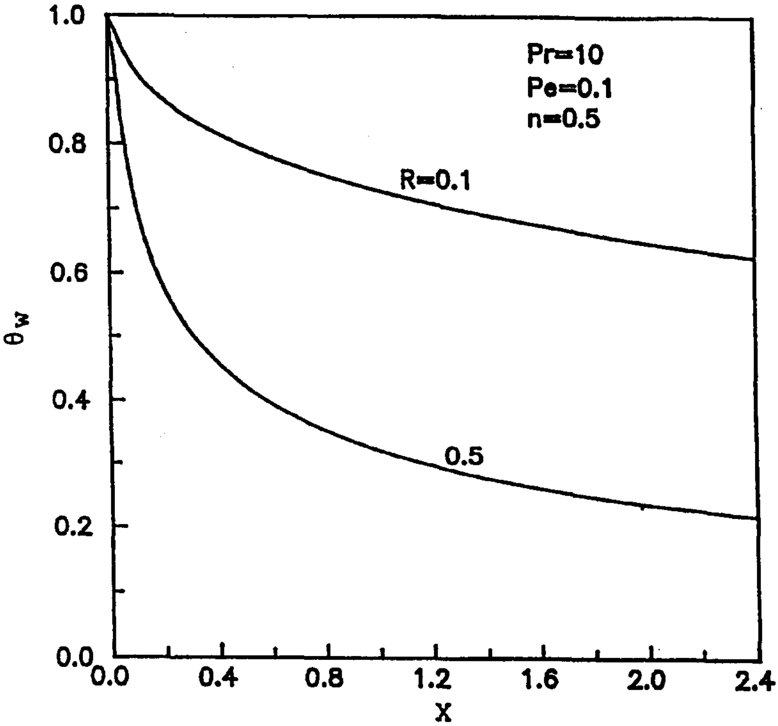


Figure 7. Effect of the parameter $R$ on the surface temperature distribution.

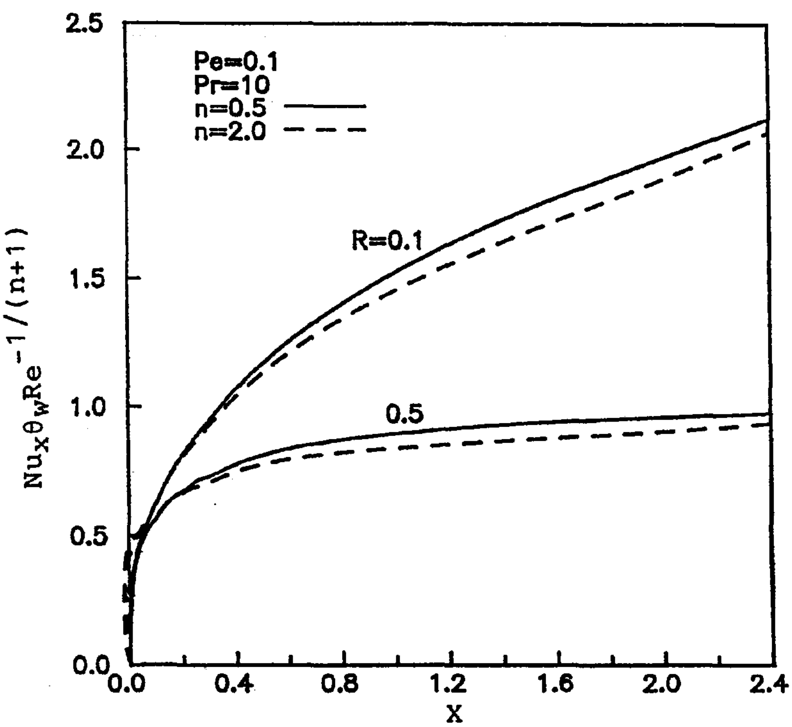


Figure 8. Local Nusselt number for different parameters $R$.

for dilatant fluids. The pseudoplastic fluids exhibit higher Nusselt number in the region far from the slot. For each fluid, the Nusselt number is observed to approach asymptotically a constant value as the distance from the slot increases. An increase in the value of the Prandtl number results in an increase of the Nusselt number for each fluid. Further, it is found that a distinctively different friction factor distribution is observed for the present fluids.

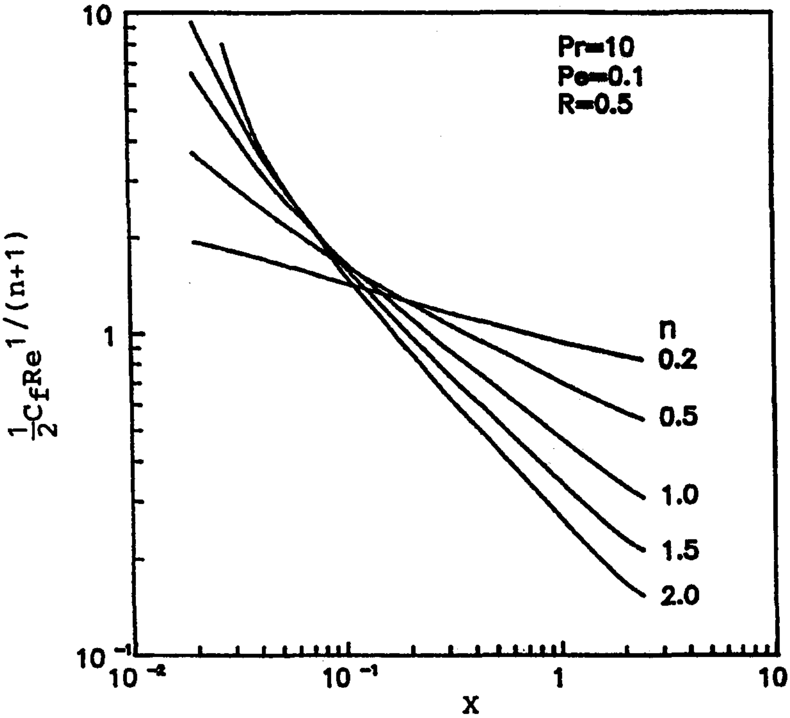


Figure 9. Effect of the viscosity index on the friction factor.

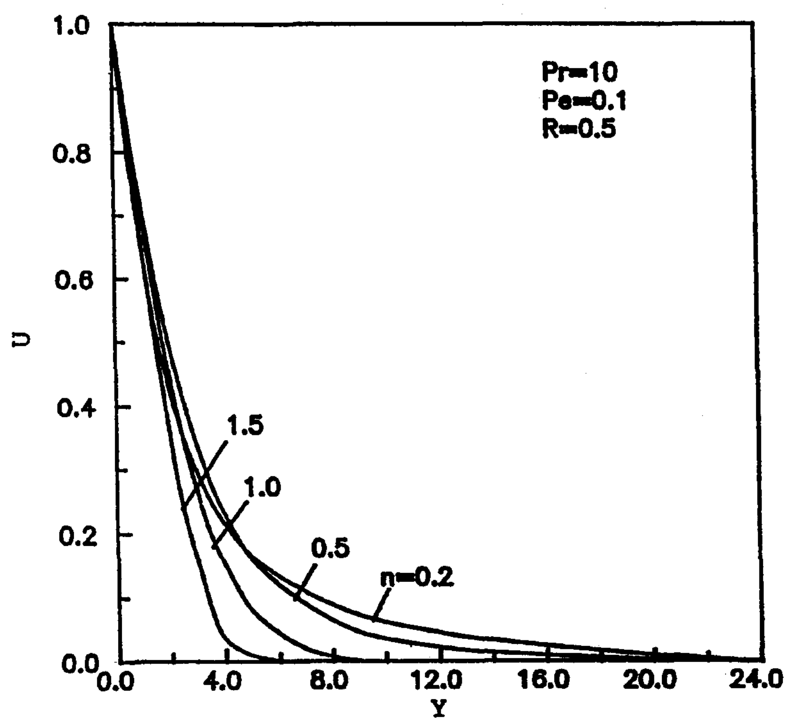


Figure 10. Velocity profiles for different viscosity indices $n$ at $X = 2.4$.

## REFERENCES


1. B.C. Sakiadis, Boundary-layer behavior on continuous solid surfaces: I—The boundary-layer equations for two dimensional and axisymmetric flow, *AIChE Journal* **7**, 26–28 (1961).
2. B.C. Sakiadis, Boundary-layer on continuous solid surface: II—The boundary-layer on continuous flat surface, *AIChE Journal* **7**, 221–225 (1961).

3. B.C. Sakiadis, Boundary-layer behavior on continuous solid surface: III—The boundary-layer on continuous cylindrical surface, *AIChE Journal* **7**, 467–472 (1961).
4. F.K. Tsou, E.M. Sparrow and R.J. Goldstein, Flow and heat transfer in the boundary layer on a continuous moving surface, *Int. J. Heat Mass Transfer* **10**, 219–235 (1967).
5. T.S. Chen and F.A. Strobel, Boundary effects in boundary layer adjacent to a continuous, moving horizontal flat plate, *Trans. of The ASME, J. of Heat Transfer* **102**, 170–172 (1980).
6. A. Moutsoglou and T.S. Chen, Boundary effects in boundary layers on inclined, continuous, moving sheets, *Trans. of The ASME, J. of Heat Transfer* **102**, 371–373 (1980).
7. L.E. Erickson, L.C. Cha and L.T. Fan, The cooling of a moving continuous flat sheet, *AIChE Chemical Engineering Process Symposium, Eighth National Heat Transfer Confenrece* **62** (64), 157–165 (1965).
8. L.J. Grubka and K.M. Bobba, Heat transfer characteristics of a continuous stretching surface with variable temperature, *Trans. of The ASME, J. of Heat Transfer* **107**, 248–250 (1985).
9. K. Chida and Y. Katto, Conjugate heat transfer of continuously moving surfaces, *Int. J. Heat Mass Transfer* **19**, 461–470 (1976).
10. M.V. Karwe and Y. Juluria, Thermal transport from a heated moving surface, *Trans. of The ASME, J. of Heat Transfer* **108**, 728–733 (1986).
11. M.V. Karwe and Y. Juluria, Fluid flow and mixed convection transport from a moving plate in rolling and extrusion processes, *Trans. of The ASME, J. of Heat Transfer* **110**, 655–661 (1988).
12. M.I. Char and C.K. Chen, Temperature field in non-Newtonian flow over a stretching plate with variable heat flux, *Int. J. Heat Mass Transfer* **31** (5), 917–921 (1988).
13. I. Pop, M. Kumari and G. Nath, Non-Newtonian boundary layers on a moving cylinder, *Int. J. Engng. Sci.* **28** (4), 303–312 (1990).
14. I. Pop and R.S.R. Gorla, Second-order boundary layer solution for a continuous moving surface in a non-Newtonian fluid, *Int. J. Engng. Sci.* **28** (4), 313–322 (1990).
15. S.G. Rubin and R.A. Graves, Viscous flow solution with a cubic spline approximation, *Computers and Fluids* **3**, 1–36 (1975).